Progress In Electromagnetics Research B, Vol. 89, 157–175, 2020

Modeling of Radiation Source Using an Equivalent Dipole Moment Model

Remya Ramesan and Deepa Madathil*

Abstract—To ensure better performance of modern electronic systems with electromagnetic compatibility (EMC) compliances, the reduction of electromagnetic interference (EMI) between modules or components of an integrated circuit (IC) is necessary. This can be achieved by developing a near field (NF) coupling model of radiating source and victim using analytical, experimental, or numerical simulation techniques. The accurate modeling of a radiation source can be performed using an array of elementary dipole moments obtained using near-field scanning measurement. This paper discusses the various techniques used in the equivalent dipole moment model to reduce the complexity and simulation time and at the same time increase the accuracy and reliability.

1. INTRODUCTION

To meet the continuously-growing needs for system integration and high density, three-dimensional integration to create multilayer chips (3-dimensional intergrated circuits) has become increasingly important, where through-silicon via is an enabling technology that provides connectivity between active layers. Network on Chip (NoC) and System on Chip (SoC) integrated circuits (ICs) are emerging technologies to meet miniaturized systems on a single chip. Intra-system electromagnetic compatibility problems are becoming very critical in this scenario. An IC can act as a real radiating noise source in an electronic system and produce electromagnetic interference in several ways that might cause Electromagnetic Compatibility (EMC) problems. The three mechanisms of coupling disturbances out of an IC are [1]:

- Conducted emission generated by each pin of IC.
- Emissions caused by an electric or magnetic near field and by internal RF voltages and RF currents of IC.
- Direct radiation caused mainly by package lead frame and bonding interconnections generated at frequency 1 GHz and above.

The analysis of EMC during the design phase of high-speed electronic circuits has become very significant recently due to an increase in working frequency and miniaturization of devices. The direct simulation of the entire IC is not possible in full-field solvers due to its complexity. Hence we focus on the accurate modeling of radiating sources by equivalent models that help in near field coupling estimation.

Thevenin or Norton source model that calculates the noise voltage and current of any device for the noise analysis is a basic approach of noise source modeling. However, the circuit analysis of the radiating source (IC) required actual manufacturing details or other information that is the intellectual property of the IC suppliers. Later source reconstruction method (SRM) or equivalent magnetic/electric current source model for characterizing the electromagnetic emission from an electronic device was studied.

Received 21 October 2020, Accepted 7 December 2020, Scheduled 15 December 2020
* Corresponding author: Deepa Madathil (deepa.m@vit.ac.in).
The authors are with the School of Electronics Engineering, Vellore Institute of Technology, Vellore, Tamil Nadu, India.

In [2], the SRM technique composed of both electric and magnetic currents is represented by a set of Rao-Wilton-Glisson basis functions. The magnetic near field data were the input information, and magnetic field integral equation was used to find the unknown coefficients of currents. The drawback of the source reconstruction method was that the size of current sources may be larger than IC and hence difficult to import into a full-wave simulation tool. Recent research has confirmed that the equivalent dipole moment model is most approximate when multiple nearby interactions co-exist. An advantage of the dipole moment source model is that it is a versatile physics-based model and does not require the the knowledge of internal circuit geometry.

According to the multipole expansion theory, any radiating source can be represented by a set of equivalent electric and magnetic dipoles which radiate the same electromagnetic field as that of a source. To develop the equivalent dipole moment model, the value of current associated with each dipole is obtained by extracting data from simulation tools like Ansys-high-frequency structure simulator (HFSS) or near-field (NF) measurements. The field of electromagnetic radiation emitted from any radiating source (antenna) can be measured in either near-field or far-field region [3]. The Friis transmission equation can be used to estimate the induced noise power at the RF antenna port when the noise coupling occurs in the far-field region [4]. However, the NF measurement has various advantages over far-field measurements including accuracy, reliability, costs, and application range. NF measurement can be done mainly by two methods such as transverse electromagnetic (TEM)/gigahertz transverse electromagnetic (GTEM) cell or Open area test (OATS) and near field scanning [1]. In [5], a source model for a test IC was extracted from GTEM cell measured at 24 rotation angles, and a set of three dipole moments including the relative phase was measured. Test IC was operated at two different operating conditions to study the effect of the victim source size on modeling accuracy. Also, the modeling and validation were done for a real application processor in a specially designed mobile product that showed reasonable accuracy. The TEM/GTEM cell method requires designing of dedicated test board that precisely fit into the input ports of the TEM cell. The design and implementation of this process leads to additional cost. Besides, the placement of complex ICs with many pins onto the limited space of a test board is a complex task. NF scanning enables the testing of radiating sources in controlled surroundings with less space. NF scanning has been a popular technique that is verified to be very effective and accurate in identifying noise sources and/or coupling paths [6].

The near field coupling estimation between radiating source and victim structure can be performed by analytical coupling models, numerical simulations, or experimental methods. There are three analytical coupling formulations such as Taylor, Agarwal, and Rachidi models that can be used to evaluate the coupled voltage between the emission source and a victim transmission line. Based on computational electromagnetic, there are various methods of modeling such as the method of moments (MoM), finite element method (FEM), finite difference method (FDM), partial element equivalent circuit model (PEEC), and transmission line matrix method (TLM). The 3-D numerical electromagnetic wave simulators such as Computer Simulation Technology (CST), Ansys-HFSS (High-Frequency Structure Simulator), FEKO, WIPL-D, IE3D, and Sonnet have proved very useful in modeling which help us to estimate the EMI during the early design phase. In [7, 8], effort was made to model the equivalent dipole moment model of EM emission in commercial electromagnetic software, such as HFSS and CST Microwave Studio. The steps involved in the insertion of the radiation emission model to commercial tool HFSS as current lines were explained in [7]. In [9], the simulation of EMI radiation from a 208 Mz single-ended I/O clock generated from SoC in an electronic device as a typical example showed a correlation within $+/-3$ dB for measured and simulated result.

This paper is a review of different methods of dipole moment model extraction examining the application of near field coupling and its contribution to EMI estimation in the Internet of Things (IoT) devices, vehicle automation, Network on Chip (NoC), and System on Chip (SoC) ICs, etc. The most important step in the extraction of equivalent dipole moment associated with an electronic device is the measurement of E-field/H-field at typical scanning points using NF scanning discussed in Section 2. The various techniques implemented to improve the accuracy in the extraction of dipole moment models are also discussed.

2. NEAR-FIELD SCANNING

Near-field scanning is used for EMC applications such as radiation emission and interference analysis of an integrated circuit (IC), printed circuit board (PCB), module, component, and radio-frequency (RF) system. It can be used to reconstruct an equivalent source model of a module or component that can be modeled in a simulation tool like Ansys-HFSS [1]. The NFs are measured at one frequency at a time and normally performed in the frequency domain. The scanning is done on three principal surfaces: the planar, cylindrical, and spherical ones. The scanning technique includes measurement using one probe in point scanning, and an array of probes is used for surface scanning. There are two techniques of source reconstruction using NF scanning: equivalent current model and equivalent dipole model. The equivalent current model is based on Huygens Love's equivalence principle, and the equivalent dipole model is based on multipole expansion and source equivalence theory. There are two types of equivalent dipole models: equivalent volume and equivalent surface dipole model [11]. An automatic near-field test bench has been set up by the Research Institute for Electronic Embedded Systems (IRSEEM) for the measurement of electromagnetic emission from radiating source. An automatic NF test bench consists of an RF signal generator, a power amplifier, a directional coupler, a power meter, an external power supply, electric/magnetic probes, and a vector analyzer (VNA) [11]. The probe is connected to the three-axis robot arm controlled by the command given by PC. The cartography of the fields generated by the probe was used to determine the effect of the electromagnetic NF on device under test (DUT) and also determine the most sensitive area of interest. In [12], the application of this NF test bench was carried out to find the exact location of the noise source, and a radiation emission source model was developed. The near-field test bench, with different equipment, is described in Figure 1. Cables are used for connectivity and amplifiers for assuring a sufficient signal to noise ratio.

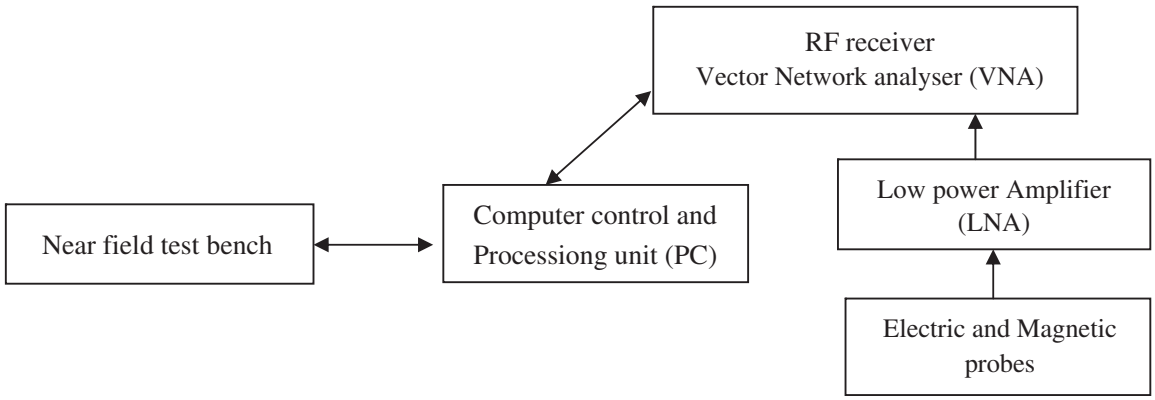

Figure 1. A basic near field scanning system.

In [13, 14], a 3-D NF measurement technique to improve the radiation emission model was used. The equivalent sources were distributed at five surfaces of a volume surrounding the DUT. It proved that 3-D modeling approach was more efficient with less measurement time for 3-D structures: a small arch device and a toroidal inductor. In the NF scanning setup, $M * M$ test points are selected uniformly from an $L * L$ mil near-field scanning plane. The scanning plane should ideally extend until the field reaches the minimum measurable level. Practically it is not necessary to scan so widely to collect enough near-field information. At every test point, the near electric and magnetic field components are measured in the selected frequency range. It is ensured that every single spot of the IC is considered and also that the number of dipoles is less than the test points [1]. The distance between the near-field probe and DUT should be very small, and a high-resolution scanning is necessary for accurately locating a noise source. Closer scanning distance leads to more accurate modeling of the radiating source and makes the solution of the inverse problem more stable. In [15], the influence of near-field scanning sizes on the accuracy of far-field estimations using a U-shape trace above a large ground plane was studied in CST Microwave Studio. The scanning area should be large enough to enclose all the radiating sources

for the specific accuracy of the far-field estimation.

An electric- or magnetic-field probe is the key of an NF scanning system that converts the field into an output voltage that can be measured. The probes are placed at a constant distance from the surface of the IC. However, often the probe response was due to the coupling of the field quantity under measurement to the probe structure. The effect of field perturbation due to probe was a function of the probe size and the distance of the probe to DUT. The perturbation created by the NF probe needs to be compensated, and hence the probe factor (PF) was defined. PF is the ratio of the field component strength it detects to the output voltage of the probe.

The vector/spectrum analyzer measures the magnitude and phase information of NF data to obtain a stable equivalent dipole source model. The challenge was in measuring phase information in practical NF scanning measurement. A reference signal is used to measure the phase, which is determined by measuring the relative phase between the fields at different locations. Most often this reference signal was chosen from the DUT, either with a touching probe or with a second probe that is placed in a strong radiation region. The easiest way is to use VNA's external reference function. However, VNA is not always affordable, so an alternative was proposed using a spectrum analyzer that was commonly used in laboratories. In [12], a spectrum analyzer together with a hybrid-coupler was used to measure the phase. The phase of the signal was obtained through three times of sweeps. The first scan captured the amplitude of the scanned signal. In the next scan, the additional power of the scanned signal and reference signal was measured through a hybrid-coupler. Finally, a known phase adjustment was applied to obtain the phase difference. This method was more complicated, time-consuming, and inaccurate. In [16], a spectrum analyzer was used to obtain the required magnetic field by measuring the electric field over the DUT, and the voltage over the surface of DUT was measured by a probe and transformed into electric field.

Yet another approach is to perform the scanning of the electromagnetic fields in the time domain (TD). Zhang et al. [17] proposed a fast and efficient calibration of the probe using the Fast Fourier Transform (FFT). The advantage of the TD approach was that phase retrieval was possible without VNA or complicated 3 sweep measurements used in [12]. Also, the measurement time was reduced because the complete frequency range could be captured in a single-shot waveform. Another advantage was that the same measurement setup could be used for calibration as well. The disadvantage of a low S/N ratio of time measurement approach was resolved by a low-noise amplifier (LNA) used after the probe output.

Due to unavoidable drawbacks in NF phase measurement especially at high frequencies, much research has been carried out for phaseless scanning. Zhao et al. [18] proposed an approach for the prediction of a radiated emission model using amplitude-only near field measurement. M_x and M_y components of magnetic dipole moments from magnetic NF measurement were used to develop the model.

In [19], two approaches to extract the model were proposed and validated using a test IC. According to the first approach, the nonlinear least square (NLS) fitting method was utilized to extract the dipole solution using the magnitude of field data [20]. For the second approach, the phases of the fields were calculated by measuring the amplitude data at two different heights, and its phase difference gave the phase information that was used to extract the model. The proposed models using two approaches were compared by taking a phase-locked loop (PLL) IC with and without shielding. It was observed that the second approach showed a better solution in both IC alone and IC shielded with metal case conditions.

In contrast to [19], Shu et al. [21] proposed source reconstruction with a single near field scanning plane. The scanning field on the single plane was divided into two groups: the sampling group and interpolation group. The sampling group was obtained by measuring the magnitude of the magnetic field and the interpolation group by the interpolation method. Each interpolation point was surrounded by four sampling points to ensure that the interpolation point could be obtained as the average of surrounding sampling points. The scanning time was reduced to half compared to [19]. The illustration of the iteration process on a single scanning plane is shown in Figure 2.

The iteration started with the initial phase is assumed as 0 rad. The first generation of the equivalent dipoles was obtained by solving the matrix equation with assumptive phase information. To nullify this assumption and to increase accuracy, a relative error (o') between the magnetic field in the interpolation group and the equivalent dipole model was calculated. The magnetic field at interpolation points was

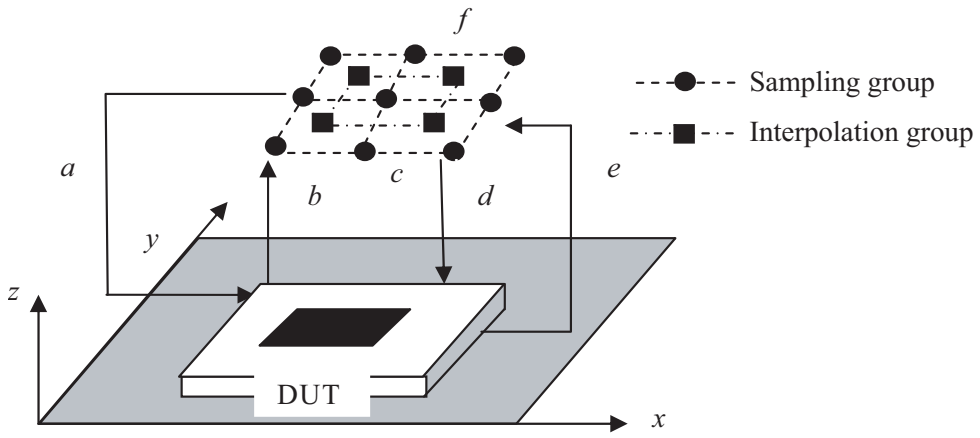

Figure 2. Sampling and interpolation points on a single plane [21].

obtained by combining the phases calculated from the equivalent dipole model and magnitude calculated at the interpolating group. Finally, the second generation of the equivalent dipole model was solved, and o' was calculated for the next generation. The iteration was repeated until o' reached the maximum average relative error defined by the user.

3. DIPOLE MOMENT MODEL

Any arbitrary electrically small radiating source can be approximately replaced by six dipoles: three electric dipoles along x, y, z directions and three magnetic dipoles along x, y, z directions, which are denoted as P_x, P_y, P_z and M_x, M_y, M_z, respectively [22]. An IC being represented as an array of equivalent dipoles that radiate the same EM fields as that of the original IC under study is illustrated in Figure 3 [23]. Any current-carrying wire can be represented as a Hertzian dipole, also referred to as a dipole moment source. The electric dipole is assumed as a linear straight electric wire and the magnetic dipole as an electric loop with a constant current.

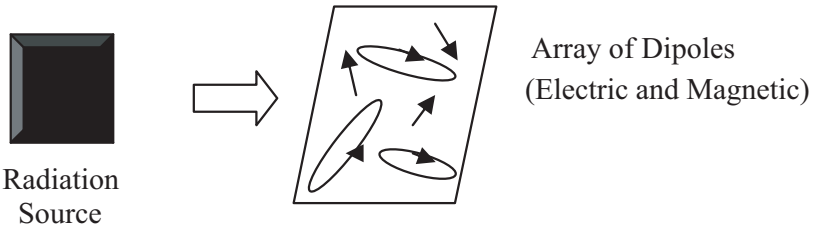

Figure 3. Equivalent dipole model representing IC.

The initial approach of radiation source modeling was 2-dimensional taking into consideration that the IC is relatively thin placed on an XY-plane. Theoretically, it is possible to represent the radiated source model entirely with electric dipoles or entirely with magnetic dipoles. In [24], two different approaches to modeling radiation sources were considered: a set of magnetic dipoles and a set of electric dipoles. According to the first approach, the IC was replaced by equivalent magnetic dipoles alone. It was possible to obtain the magnetic dipoles by measuring the NF scan of only one component of the magnetic field at a certain distance close to the DUT. To build the model, the expressions of the magnetic field [H_x, H_y, H_z] radiated by an elemental magnetic dipole were used. The orientations of the dipoles were fixed, and the amplitude and phase of the current that goes through each dipole were calculated. In the second approach, a set of electric dipoles was placed in the XY-plane to represent the radiating IC. The orientation of dipoles was obtained from the procedure of modeling, rather than been

fixed. This accounted for more accurate results using a set of electric dipoles than a set of magnetic dipoles. However, it required two components [H_x, H_y] NF scan to obtain the equivalent model due to the calculation of the orientation of dipoles. The magnetic dipoles approach was faster than the electric dipoles approach concerning the time of calculation.

It was observed that the simultaneous use of both electric and magnetic dipoles in the model adds redundancy to the measurements but makes prediction less prone to propagation and errors due to uncertainty in measurements. Leseigneur et al. [25] proposed a 2D model consisting of a set of equivalent electric and magnetic dipoles placed on an XY plane. The mathematical expression of the problem in matrix form is given by Eq. (1) [25],

$$\begin{pmatrix} [E_x] \\ [E_y] \\ [H_x] \\ [H_y] \end{pmatrix} = \begin{pmatrix} \propto 1,1 & \dots & \propto 1,s \\ \vdots & \ddots & \vdots \\ \propto r,1 & \dots & \propto r,s \end{pmatrix} \begin{pmatrix} I_e \sin\varphi e \\ I_e \cos\theta e \\ I_m \sin\theta m \\ I_m \cos\theta m \end{pmatrix} \tag{1}$$

where $[E_x]$,$[E_y]$,$[H_x]$,$[H_y]$ was the tangential components of electric and magnetic fields. These tangential near field components were obtained from NF measurement. The factor α_{ij} depended on factors such as frequency, length, the position of dipoles that are preliminarily fixed by the user. Also, $s/2$ was the total number of equivalent dipoles and $r/4$ the number of locations where the field was estimated. The unknown parameters were the currents I_e, I_m, and orientations θ_e and θ_m. The least-square and division element-by-element methods were used to calculate θ_e and θ_m by defining a new parameter [β] that depended on user-defined parameters and orientations. Finally, I_e, I_m are obtained from Eq. (2) [25].

$$\begin{pmatrix} [E_x] \\ [E_y] \\ [H_x] \\ [H_y] \end{pmatrix} = \begin{pmatrix} \beta 1,1 & \dots & \beta 1,s/2 \\ \vdots & \ddots & \vdots \\ \beta r,1 & \dots & \beta r,s/2 \end{pmatrix} \begin{pmatrix} [I_e] \\ [I_m] \end{pmatrix} \tag{2}$$

The extracted electric and magnetic dipoles that represented the emission source were modeled in commercial electromagnetic software such as HFSS. It was observed that when complex devices are to be modeled in full-wave simulators, the reduction in dipole number was necessary. For this, two threshold electric and magnetic currents were defined. The electric and magnetic currents greater than the threshold were kept in the reduced model. This resulted in a decreased insertion time and less computer memory for simulation.

In [26], the proposed model differs slightly from [25] in terms of the variable parameters associated with the equivalent source model. [25, 27] used θ_e, θ_m, I_e, and I_m to describe the magnitude and direction of currents at a fixed set of predefined locations of allied dipoles. However, in the proposed model, the variables associated with the set of dipoles were denoted by I_{ex}, I_{ey}, I_{mx}, and I_{my} obtained using single matrix inversion. The orientation of the electric and magnetic dipoles was fixed, and thus the only parameter to be solved was the electric and magnetic current. The methodology was verified by HFSS simulation as well as NF scanning measurements through application to a micro-strip hybrid. The field components (E_x, E_y, H_x, H_y) at a certain distance (2 mm above the hybrid) were used to model the equivalent source using HFSS and NF scanning. The required electromagnetic fields were calculated in Matlab. The results from direct HFSS simulation and the equivalent model were compared and showed that the error was less than 5%.

Later, Shall et al. [28] proposed a 3-dimensional modeling process for counting the real-world scenario in power electronic devices. The 3-D model was based on an array of elementary dipoles on the five faces of a six surface volume around the 3-D arc (radiating source). The sixth face was not considered as it was the ground plane of the DUT. The cartographies of E/H-fields necessary to extract the model were obtained directly from simulation on HFSS. The 3-D modeling procedure proved more efficient and accurate with fewer dipoles than the 2-D model presented in [25]. The 3-D modeling approach was first presented in [28] and further investigated in [10] to predict the EMI between complex electronic devices and interconnections. In [10], a model was built in HFSS with fewer dipoles using electromagnetic field components extracted from magnetic NF measurement. It required four tangential field components for measurement points for each considered surface to develop the model. The five

planes and their EM fields were defined as follows: 1) XY plane — $[H_{x1}, H_{y1}, E_{x1}, E_{y1}]$, 2) XZ_2 plane — $[H_{x2}, H_{z2}, E_{x2}, E_{z2}]$, 3) YZ_3 plane — $[H_{y3}, H_{z3}, E_{y3}, E_{z3}]$, 4) XZ_4 plane — $[H_{x4}, H_{z4}, E_{x4}, E_{z4}]$, and 5) XZ_5 plane — $[H_{x5}, H_{z5}, E_{x5}, E_{z5}]$. The proposed 3-D model proved to be more accurate and required fewer dipoles than the 2-D NF model described in [25–27].

Further study of noise source as working IC discovered that it is normally placed very close to the ground which can be deemed as perfect electric conductor (PEC) boundary condition. The contribution of a vertical magnetic dipole, the tangential electric dipole, and its images cancel each other. Thus M_x, M_y, P_z become dominant dipole moment, and it can successfully represent a radiating IC source [22, 29–33] depicted in Figure 4. The P_z dipole will represent the voltage distribution between the IC and ground plane, and M_x, M_y dipoles represent the current distribution of IC. In [31], this idea was utilized, and each elemental point dipole was decomposed into M_x, M_y, P_z. The near field measurement data $[E_x]$, $[E_y]$, $[H_x]$, $[H_y]$ were used to calculate the magnitude and phase of dipole sources. The electromagnetic fields radiated by dipoles, in this case, are calculated by Eq. (3) [31],

$$\begin{pmatrix} [E_x] \\ [E_y] \\ [H_x] \\ [H_y] \end{pmatrix} = T \begin{pmatrix} [P_z] \\ [M_x] \\ [M_y] \end{pmatrix} \tag{3}$$

T was the field generation matrix and expressed by Eq. (4) [31],

$$T = \begin{pmatrix} T_{E_xP_z} & T_{E_xM_x} & T_{E_xM_y} \\ T_{E_yP_z} & T_{E_yM_x} & T_{E_yM_y} \\ T_{H_xP_z} & T_{H_xM_x} & T_{H_xM_y} \\ T_{H_yP_z} & T_{H_yM_x} & T_{H_yM_y} \end{pmatrix} \tag{4}$$

The proposed model was validated by a radiating trace on a metal plane filled with air in a 3-D full-wave simulation tool. The dipole moment model was calculated in simulation from NF measurement

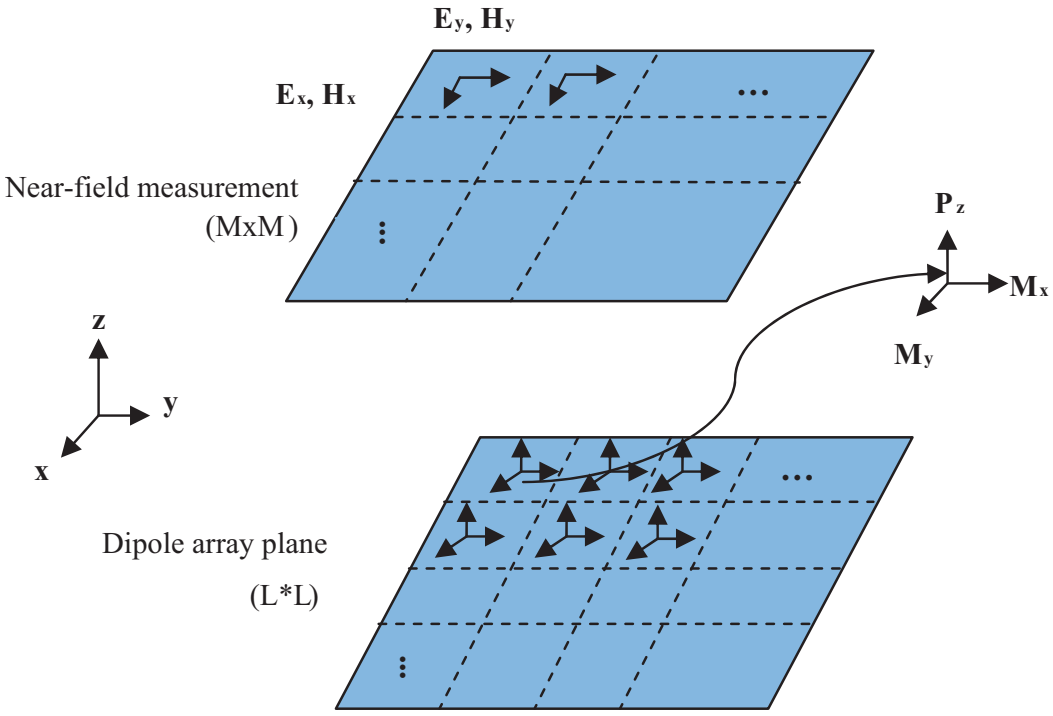

Figure 4. Equivalent source model using a dipole array [30].

using the inverse method. Also to improve the numerical stability, the regularization technique was implemented.

Tong et al. [32] also proposed a model similar to [31], while considering PCB in an open and closed environment. The PCB was modeled inside an enclosure in which case we need to characterize the interaction between PCB and the enclosure. A dipole-dielectric conducting (DDC) plane model was illustrated which consists of a dielectric layer and horizontal electric dipoles for the active excitation. The basic features such as ground plane and substrate were added to the equivalent dipole model that resulted in the accurate modeling of emission source in free space and also within an enclosure. It was validated that the magnetic dipole model gave a better solution than the electric dipole model. This was because the inverse problem associated with the electric dipole model was unstable and sensitive to noise. The dipole stability could be improved by suppressing the perturbation influence of the measurement error in NF data which was achieved by regularization algorithms. Hence in the proposed model, the Tikhonov regularization scheme was implemented which was the standard for mitigating the ill-conditioning of the inverse problem. It was also found that the error of the dipole solution was affected by the condition number of transfer matrix that was influenced by the number, the distributions, and the locations of the dipoles and scanning points. So the effort was made to reduce the sensitivity of measurement error by decreasing the condition number in the inverse problem matrix. This was achieved by setting an optimal scanning resolution and area that reduced the number of dipoles and by selecting scanning distance as minimum as possible. The relative error between the modeled field and simulated field in a validation plane was about 3 percent, and hence this proved the clear physical meaning of the model.

Differing from [31, 32], [22, 29] used the tangential magnetic fields [H_x, H_y] for extracting the M_x, M_y, P_z set of dipoles at each point on the scanning plane. The magnetic field radiated from dipoles is calculated by Eq. (5) [22, 29],

$$\begin{pmatrix} [H_x] \\ [H_y] \end{pmatrix} = T \begin{pmatrix} [P_z] \\ [M_x] \\ [M_y] \end{pmatrix} \tag{5}$$

T is the field generation matrix and expressed by [22, 29],

$$T = \begin{pmatrix} T_{H_xP_z} & T_{H_xM_x} & T_{H_xM_y} \\ T_{H_yP_z} & T_{H_yM_x} & T_{H_yM_y} \end{pmatrix} \tag{6}$$

The field generation matrix T was related to the location of observation points, location of source points, frequency of operation, and also type, orientation, and the number of dipoles. After normalization, the relationship between dipole moment sources and radiated fields is given by Eq. (7) [29],

$$F_n = T_{nk} X_k \tag{7}$$

The dipole solution vector X_k denotes the dipole sources, T_{nk} the normalized form of field transfer matrix, and F_n the tangential and normal electromagnetic field components after normalization. The least-square was now used to reconstruct the model using a solution given by Eq. (8) [29],

$$X_k = [T'_{nk} T_{nk}]^{-1} T_{nk} F_n \tag{8}$$

where T'_{nk} is the conjugate transpose of T_{nk}. X_k determines the actual dipole moments. In [29], the least square (LSQ) method minimized objective function defined as [29],

$$H = \|F_n - T_{nk} X_k\|^2 \tag{9}$$

The number of dipoles may be large depending upon the dimension of DUT which may lead to an overfitting problem. The singular value decomposition (SVD) method was used for reducing the effect of ill-conditioning, ensuring the quality and sufficiency of the NF data. The regularization coefficient was used to adjust the weight of the stability and accuracy of the solution source matrix and was obtained by methods such as "L-Carve", intelligent optimization algorithm, generalized cross-validation, machine learning, and truncated singular value decomposition (TSVD). The selection of an appropriate regularization coefficient was difficult when the error level was not clear, and the transfer matrix had a large scale. Also, the regularization iteration steps could be time-consuming for complex transfer matrix.

When the regularization could not converge rapidly, the number of iteration steps increased [34]. Taking this into account, Tan et al. [35] proposed a hybrid method for dipole model extraction from near field scanning based on regularization and TSVD method. A differential pair was modeled to validate the proposed model and proved successful in improving noise issues. The main objective of the regularization technique was to minimize the total energy of the dipole sets, and the function was redefined as [30],

$$H_{redefined} = \|F_n - T_{nk}X_k\|^2 + \lambda^2\|X_k\|^2 \tag{10}$$

where λ is a regularization coefficient; $\|F_n - T_{nk}X_k\|^2$ determined the accuracy of the solution, and $\lambda^2\|Xk\|^2$ minimized the total energy of the equivalent sources. The regularized solution is written as [30],

$$X_k{}^{\text{reg}}(\lambda) = \left[T'_{nk}T_{nk} + \lambda^2 I\right]^{-1} T'_{nk}F_n \tag{11}$$

I was the identity matrix; regularization coefficient λ was used to adjust the weights of the two terms. An alternate method was the truncated SVD method based on singular value decomposition of the matrix T_{nk} given by Eq. (12) [30],

$$T_{nk} = U\,S\,V' \tag{12}$$

V and U are $K*K$ and $L*L$ unitary matrices. V' is the conjugate transpose of V. S is a $K*L$ matrix whose diagonal elements were the singular value of T_{nk}. Thus the solution of the $TSVD$ method is written as Eq. (13) [30],

$$Xk^{TSVD}(r) = V_r \begin{pmatrix} s_{11}^{-1} & \cdots & \\ & \ddots & \\ & \cdots & s_{rr}^{-1} \end{pmatrix} U'_r \quad F_n \tag{13}$$

Xk^{TSVD} denotes the TSVD value of X_k. V_r is an $L*r$ matrix from the first r columns of V, and U_r is a $K*r$ matrix from the first 'r' columns of U. Also 'r' is the number of the larger singular values kept unchanged. The improved source model with $TSVD$ and regularization technique proved very accurate to evaluate near fields and also in modeling far-field emissions.

Near-field plane data from the scanning technique consisted of some perturbations or interferences. The stability of the equivalent model depended on the condition number of the mapped matrix and the interference level in the NF scan data [33]. This was mathematically defined as, if $F = F^e + \Delta F$, $T = T^e + \Delta T$ and $X = X^e + \Delta X$, then Eq. (7) can be rewritten as [33],

$$(T^e + \Delta T)(X^e + \Delta X) = (F^e + \Delta F) \tag{14}$$

The superscript 'e' denotes value without interference. ΔF denotes interference in field strength data. ΔT denotes the error from the mapped matrix due to truncation error, and it could be reduced by double-precision floating-point operands. ΔX denoted the dipole moment error due to ΔF. Now the interference in field transfer matrix (T) and errors of regularization solution are calculated by Eq. (15) [33],

$$||X^{re} - X|| / ||X|| < \text{cond}(T)\,\|F - TX^{re}\| / \|F\| \tag{15}$$

The condition number of T, $\text{cond}(T) = \|T\| \cdot \|T^{-1}\|$ and $\|\cdot\|$, denotes the Euclidean vector norm. The superscript 're' denotes the solution using the regularization technique. The regularization procedure helped to extract the equivalent source model not sensitive to such interferences and solved the inverse problem without the known condition number. Liu et al. [33] proposed the regularization solution with different mapped matrices and tested whether the regularization solution would change significantly with interference added in the field strength data. It was observed that condition number and relative error increased with increased dipole number, and stability of the solution was strongly related to the field transfer matrix. It was also seen in the simulated result that cond(T) and relative error were reduced with increased scanning point intervals. A large dipole array represented the radiated field more precisely with decreased relative error. However, the number of dipoles cannot be set very high to ensure the unique solution. The stability and accuracy of the equivalent model cannot be achieved simultaneously. Hence, a trade-off was needed in the selection of a mapped matrix to extract the radiation model accurately.

The dipole array equivalent model was mostly used in the frequency domain (FD). However, there were a few publications using time-domain (TD) approach as well [36–40]. These aforementioned researches applied the finite-difference time-domain (FDTD) method which was computationally inefficient for complex structures like PCB. To overcome this challenge, Ravelo et al. [41] proposed the time-domain (TD) model using an array of elementary electric dipoles. This approach precisely analyzed the variation of the NF emission level at every critical time instant. Hence, it proved to be very useful for the EMC prediction in modern multifunction analog-digital systems with multiple digital clocks, RF transmitters, etc. TD model could be extracted by analysis, simulation, or measurement with transient perturbations in the radiating planar structure. The electric dipole moment components were calculated using linear matrix inversion with a suitable numerical method for time-sampled functions. It was exported to a full-wave simulator, and validation with transient NF radiation was studied. The model was less accurate at more distance from the dipole plane due to wave propagation delays. On the other hand, as the distance from the scanning plane increased, disturbances due to the scanning probe and quasi-static assumption effect were reduced. The model was validated by developing an equivalent model consisting of a set of electric dipoles from the analytical calculation in MATLAB. It was further verified by measurement using a passive microstrip structure and proved the efficiency of the TD model. Later Liu et al. [42] proposed a magnetic dipole array based on a time-domain(TD) approach well suited for circuits with clear current loops, e.g., loop antennas and spiral inductors. A comparison of electric and magnetic dipole based TD models was carried out using two microstrip structures, a straight microstrip (I-line) and a microstrip loop with 1040 elementary dipoles in CST. It was proved that the electric dipole TD model was more accurate at height $z = 10\,\text{mm}$, and the magnetic dipole TD model performed well for larger height, say $z = 25\,\text{mm}$.

Zhang et al. [17] proposed a hybrid method to simulate electromagnetic emission from PCB based on an array of dipoles from NF measurement imported into a finite time difference domain (FDTD) calculation space. The tangential magnetic field distribution from the NF scan was used to obtain the tangential magnetic field component, orientation, magnitude, and phase of the dipoles. The calculation space of the FDTD algorithm was a mesh of Yee cells, and the UPML (uni-axial anisotropic perfectly matched layer) boundary was considered. FDTD algorithm proved to be very effective and efficient in EMI prediction of PCB with shielding.

We understood that as the number of dipoles used in the equivalent model increased, the time consumed for its simulation also increased. The focus was now given on how to reduce the number of dipoles while designing complex electronic products. Huang et al. [43] proposed a transfer function based dipole model that made it more scalable. According to the proposed model, a one-time simulation of the model was required, and this result was used to construct the transfer function of a similar structure. The simulation results obtained at one-time were used to construct transfer functions. This transfer function was reused in other cases, with a change in some parameters of the noise source that reduced the engineering time. A full-wave simulation model of noise source and victim antenna was used to obtain a set of transfer functions. The complex product of the transfer function and the complex value of the dipole moment produce the coupled voltage of the dipole moment at every test point. The total coupled voltage was the linear summation of these coupled voltages. A test board with two patch antennas was used to validate the proposed model, and an error less than 3 dB between predicted and measured results was obtained.

Zhang et al. [44] proposed a hybrid source reconstruction method to overcome the lack of flexibility of [35] by managing different working conditions of the IC. It consisted of two groups of equivalent dipoles and made a physical relationship to inbuilt electrical properties of IC. The first set of dipoles represented radiation from lead-frame pins and bonding wires by converting the current/voltage distribution of IC's package into equivalent electric and magnetic dipoles. The current/voltage was obtained by measurement or circuit simulation. The second set of dipoles represented radiation from the die and the lead-frame flag beneath the die and was solved by LSQ and regularization techniques. The second set was also adjusted by scaling to adapt to varying operating conditions. The scaling factor was a change ratio of new current flowing to the previous currents in the power/ground pins under the changing working conditions. Finally, the hybrid emission model was obtained by adding the two sets of dipoles. For the validation of the flexible hybrid model, a commercial 8-bit microcontroller used in the washing machine at three working conditions such as core program and port program modes was simulated in

HFSS.

Huang et al. [45] proposed a method of source reconstruction using a machine learning algorithm that was found better than the conventional LSQ method of the dipole moment model. An algorithm was developed with a training set developed for the six basic dipole moments (P_x, P_y, P_z, M_x, M_y, and M_z). The algorithm was capable of extracting the primary dipole moment of complicated field patterns after training. The location of the dipole moment was determined by autocorrelation. The magnitude and phase of the dominant dipoles were extracted using the LSQ method. Once the first and most dominant dipole moment was extracted, a new field pattern was generated by subtracting the original field pattern and the field pattern of the first dipole moment. This process was repeated on the newly obtained field pattern. When the difference between the field pattern from the extracted dipole moment and measurement met a certain criterion or the maximum iteration number, the iteration was stopped. Thus the most dominant dipole moments for the noise source were extracted one by one. The proposed method was validated using a test board, and a practical cell phone showed better accuracy and reliability.

Further research was carried out to improve the equivalent source model with the utmost accuracy. Benyoubi et al. [46] proposed a radiation emission model based on elemental magnetic dipoles from magnetic near field measurement. The proposed method was a combination of two earlier approaches; optimization algorithm was used to determine the position of dipoles, and the matrix inversion method was used to get the respective dipole moments. The magnetic field cartographies were obtained using magnetic probes in near field test bench setup. To reduce the unknown parameters, dipoles in a finite volume were considered. Initially, the algorithm started with a single dipole moment and randomly selected position parameter. The magnetic field measurement in the field created by dipoles and calculated by analytical equations was compared, and their difference was defined as a fitness function. The minimization of the fitness function was done by incorporating a genetic algorithm combined with a pattern search using the Matlab Optimization toolbox. The difference between the fitness functions of two consecutive numbers of the dipoles was calculated, and the optimization iteration was stopped when this difference was less than a threshold defined by the user. The NF magnetic measurements were performed, and the equivalent magnetic dipole model of a mono turn coil, a toroidal coil, and a complex case (dc/dc converter) were simulated in HFSS and proved that the number of dipoles and computation time were reduced by this approach.

Later Wu et al. [47] proposed a new approach based on genetic algorithm and LSQ method that significantly reduced the number of dipoles, optimization time, and was more robust. The optimization range of dipole type was the six basic dipoles (P_x, P_y, P_z, M_x, M_y, M_z), and the optimization range of location was decided by the size of the radiating source. The proposed algorithm consisted of the following steps: (a) Dipole type and location were randomly decided by the user. (b) LSQ method was used to obtain the magnitude and phase of dipoles. (c) Then the relative error was calculated between the scanned field and calculated field. (d) The subsequent generations were evolved by selection, crossover, and mutation of the current generation. (e) This step was iterated until the maximum generation was reached, or minimum tolerance was obtained. (f) The algorithm finally returned the optimized dipole type and location with minimized relative error. For the validation of the proposed method, near-field coupling between a clock buffer IC and an inverted F antenna as a victim was carried out. The relative error of 0.132 was obtained between the measured field and calculated field from dipoles. The model was simulated in HFSS, and a difference less than 1 dB was obtained between the simulated and measured values at different working frequencies, 1467 MHz–1733 MHz.

Due to the limitations of the tangential electric field probe, the measurement of tangential component of the electric field is difficult and time-consuming. On the other hand, a typical near-field probe can easily obtain the normal component of electric field. Considering this, Liu et al. [48] proposed a new transfer model with fewer near-field data, and the scale of the transfer matrix was also reduced. The vector F_n in Eq. (7) was reduced to only the normal component of the electric field that reduced the test difficulty and also enhanced the efficiency of measurement. The new transfer model was represented as Eq. (16) [48],

$$\begin{pmatrix} [E_z] \\ [H_x] \\ [H_y] \end{pmatrix} = T \begin{pmatrix} [P_z] \\ [M_x] \\ [M_y] \end{pmatrix} \tag{16}$$

Table 1. Summary of different dipole moment models.

Author [Ref.]	Year	Proposed Method	Numerical Validation	Advantage
Yu et al. [31]	2010	P_z, M_x, M_y dipole moments to model from [E_x, E_y, H_x, H_y] NF data. LSQ with regularization technique was used.	A radiating trace.	Extract the physical IC model.
Tong et al. [49]	2010	Magnetic dipoles (M_x, M_y, M_z) were used to develop a dipole model of PCB from [H_x, H_y] NF data.	Test board with microstrip printed on substrate, practical telemetry board.	Modeling in an open and closed environment studied.
Yu et al. [30]	2012	P_z, M_x, M_y dipole moments are used to model. Also, the regularization technique and Truncated SVD method are used for optimization.	Trace and a small patch geometry.	Improved Dipole moment model.
Zhao et al. [18]	2012	Magnetic dipoles from amplitude-only NF measurement. A Differential evolution algorithm was used to determine dipole parameters.	PCB with an L-shaped microstrip line and the ground plane.	Computational complexity is reduced.
Pan et al. [50]	2013	P_z, M_x, M_y dipole moments are used to model real IC from [E_x,E_y,H_x,H_y] NF data.	LVT16245B, a 16-bit bus transreceiver.	Radiation from heat sink excited by IC studied.
Liu et al. [10]	2013	3-D modeling with sets of electric and magnetic dipoles distributed on five surfaces of a parallelepiped surrounding the DUT	A 3 D small arc above a ground plane.	Accurate than the 2-D approach.
Pan et al. [29]	2015	Magnetic near fields [H_x, H_y] to extract the dipole model. Vertical electric dipole (P_z) and horizontal magnetic dipoles (M_x, M_y) used.	Patch antenna	Proved successful with an estimation error of less than 0.5 dB.
Ravelo et al. [41]	2015	Time-domain electric dipole model from NF scan data.	A microstrip circuit printed on the FR4 substrate.	The first step to the TD approach.
Pan et al. [51]	2016	P_z, M_x, M_y dipole moments were used to model from [H_x,H_y] NF data.	A passive structure consisting of 3 patch antenna and a short trace.	The concept of "RF Library" introduced-dipole models for different noise sources saved in "source Library".

Li et al. [22]	2016	M_x, M_y, and P_z were used for a model from [H_x, H_y] NF data. Huygen's model was also implemented.	A patch antenna	Huygen's equivalent model and equivalent dipole model were compared.
Tan et al. [35]	2016	A hybrid method based on the truncated SVD method and the regularization technique was used. M_x, M_y, and P_z from [E_x, E_y, H_x, H_y] NF scan data used for the dipole model.	A differential pair with two traces.	Accurate and provide clear physical meaning.
Liu [33]	2016	Equivalent Dipole-Moment Model using an Improved mapped matrix to account for interference in NF measurement. Regularization technique to improve the stability and accuracy of the solution.	A radiating trace in the PEC ground plane.	A stable and accurate model by selecting the best condition number.
Liu et al. [42]	2016	Time domain magnetic dipole model from NF [H_x, H_y, H_z] data.	Planar microstrip Chebyshev filter PCB	Proved TD electric dipole model has better accuracy.
Kwak et al. [52]	2017	An equivalent array of dipole moments model from only the magnitude data of near-field scan. NLS and TSVD method applied.	Dipole sources P_z, M_x, M_y at 3 different positions.	Magnitude data only reduced labor in measurement.
Zhang et al. [16]	2017	EM dipoles determined from [H_x, H_y, H_z] data of NF scan. The dipole array is imported to the FDTD calculation space.	Two areas of 4-layer PCB.	FDTD was efficient and proved a new technique of EMI prediction of PCB.
Zhang et al. [44]	2017	A hybrid model of 2 sets of equivalent dipoles and scaling factors to adapt to the varying working condition of IC.	8-bit microcontroller	The different working condition of IC was accounted for.
Tong et al. [3]	2018	Dipole moment model from GTEM cell measurement.	Test IC and real application processor on a mobile phone.	Accuracy.
Huang et al. [45]	2018	A machine learning algorithm for dipole moment model	A test board and practical cell phone.	Accurate and reliable.
Huang et al. [43]	2018	Transfer Function Based Dipole Moment Model	Patch antenna	One-time full-wave simulation and reused for other cases.
Shu et al. [21]	2018	Source reconstruction from phaseless single-plane scanning. Iteration algorithm combined with the SVD method for accuracy.	A patch antenna	Scanning time was reduced to half.

Wu et al. [47]	2019	Dipole model using genetic algorithm and LSQ method.	A clock buffer chip.	Reduces optimization time and robustness.
Liu et al. [48]	2020	The dipole model is based on a new transfer model using only [E_z, H_x, H_y] NF data. Also, regularization optimization based on Tikhonov and TSVD was used.	Delay line, microstrip antenna, the motherboard of frequency digitizer.	Enhance stability and accuracy.

To improve accuracy and stability, an accelerated iteration approach was adopted to find the optimized transfer matrix with an optimized condition number. The new transfer matrix proposed in this model was built on a multiport model in Matlab. The input variables were the number of test points (NT), number of dipoles (ND), height of near-field scanning plane (HT), height of dipole array plane (HD), and frequency of simulation (f), and output variable was condition number (CT). The accelerated method was carried out based on the gradient of CT whose value changed with different input variables. In addition, the regularization technique as in [33] was implemented to obtain the optimum dipole solution. Table 1 gives a summary of different techniques used in improving the dipole moment model.

4. APPLICATION OF EQUIVALENT DIPOLE MOMENT MODEL

The use of IoT devices connected by wireless communication makes it very convenient but at the same time makes it more vulnerable to electromagnetic interference. A radio receiver (RF antenna) can easily pick electromagnetic noise from integrated circuits (ICs) situated within the same device. Hence the radio range is often limited by EMI referred to as RF desensitization that limits the range of IoT devices. The interest in RF desensitization topic has increased recently as more and more electronic devices are moving into IoT platform. Hence, the EMI estimation using source modeling and coupling estimation associated with them using numerical simulation in early design cycle can be used as an efficient and fast tool for the design of IoT devices. A typical example is mobile phone that has multiple RF antennas offering different features like Wi-Fi, Bluetooth, GPS (Global positioning system), GSM (Global system for mobile communication), etc. which work at a wider and high frequency ranges. As a result of miniaturization of device with increasing clock speed and data rates, the components within the mobile phone such as LCD (Liquid crystal display) module, camera, and application processor can act as radiating source and cause coupling to RF antennas and to each other. Another emerging technology that needs close attention is the modern automotive industry that requires many electronic systems for control and communication placed at different parts of the vehicle connected by cables that produce radio frequency interference. The analysis of EMI and RF desensitization for wireless communication can be successfully done by our proposed source modeling and coupling estimation.

The modeling of the radiation source with the equivalent dipole moment model finds its application in near field coupling estimation. It helps us to model complex radiating structures in a full-wave simulator, and its coupling in the presence of victim structures can be easily calculated. The dipole moment model equivalently represents a radiating source and hence can be applied to noise source modeling and predesign analysis of electromagnetic interference between closely situated electronic devices. A Wilkinson power divider (passive device) and an oscillator (active device) as a noise source and a transmission line as the victim were simulated in HFSS, and the coupling voltage was calculated [25]. In [29], the application of dipole moment model for EMI estimation was validated by considering two simple patch antennas placed on the PCB designed to work at 2.5 GHz. Table 2 gives the comparison of coupling power obtained for two cases: (1) source patch antenna and victim patch antenna, (2) equivalent dipole moment model of source patch antenna and victim patch antenna that gave an estimation error of 0.5 dB.

In [51, 53–55], a combination of equivalent dipole moment model and decomposition method based on the reciprocity theorem was used for measuring the near field coupling. The reciprocity theorem for radio-frequency interference estimation was decomposed into two parts. In the first step (forward

Table 2. Comparison of coupling power by simulation [29].

Frequency	Simulating Coupling power	
	Real source to victim	Dipoles to victim
2.5 GHz	−35.00 dBm	−34.53 dBm

problem), noise source IC was modeled as equivalent dipole moment from the near-field measurement. In the second step (reverse problem), the victim antenna with a source IC removed was modeled in the full-wave simulation tool HFSS-Ansys. Huygen's surface enclosed the victim antenna to take account of the antenna of any complex geometry. Finally, the noise coupling power at the RF antenna port was calculated from the two sets of the tangential electromagnetic fields on the reference Huygen's box based on the reciprocity theorem. Figure 5 shows a comparison of coupled power using reciprocity theorem and direct measurement, and the difference between them was less than 5 dB which is acceptable.

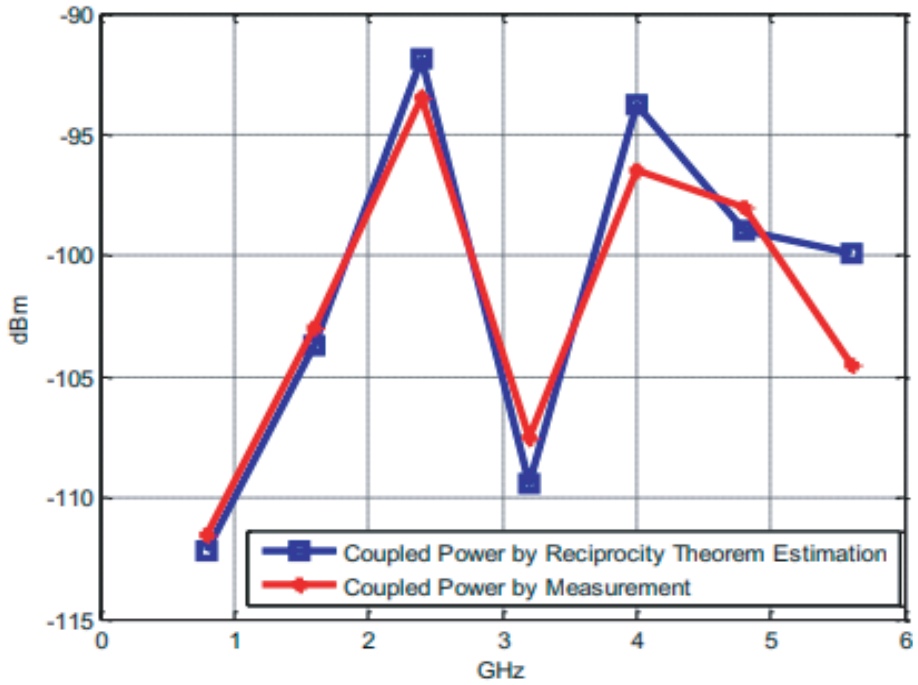

Figure 5. Coupled power by reciprocity theorem and measurement [50].

5. CONCLUSION

The dipole moment model has been observed appropriate in modeling a radiating source, typically complex ICs at higher frequencies. The equivalent dipole moment reconstruction helps in finding the physical insights of noise source from NF scan data. The future focus will be to develop techniques for eliminating scanning errors during NF measurement and determining the initial configuration of dipole sets that can improve the accuracy and efficiency of model extraction. Compared to conventional LSQ method of source reconstruction, the recent methodologies adopting such as regularization technique, TSVD method, machine learning algorithm, new transfer function model, phaseless scan, and genetic algorithm have increased the accuracy and reliability. The proposed method can be conducted at early design stage without original application board and hence will help shorten the product life cycle, cost, and time for product design. It is observed that more research can be carried out in creating an efficient

coupling model incorporating the integration of the dipole moment model with different techniques of near field coupling estimation. The analytical approach has its advantages and limitations compared to the numerical approach. So an intelligent combination of both, hybridization technique, seems a good solution to the problem of EMI in complex real world applications.

REFERENCES

1. Deutschmann, B., H. Pitsch, and G. Langer, "Near field measurements to predict the electromagnetic emission of integrated circuits," *International Workshop on Electromagnetic Compatibility of Integrated Circuits*, 2005.
2. Li, P. and L. J. Jiang, "Source reconstruction method-based radiated emission characterization for PCBs", *IEEE Transactions on Electromagnetic Compatibility*, Vol. 55, No. 5, October 2013.
3. Tong, X., "Simplified equivalent modelling of electromagnetic emissions from printed circuit boards," Ph.D. thesis, University of Nottingham, 2010.
4. Balanis, C. A., *Antenna Theory. Analysis and Design*, 94–96, 3rd Edition, Wiley, New York, 2005.
5. Kwak, K., J. Kim, and J. Kim, "Near-field validation of dipole-moment model extracted from GTEM cell measurements and application to a real application processor," *IEEE Transactions on Electromagnetic Compatibility*, Vol. 60, No. 2, 2018.
6. Weng, H., D. G. Beetner, and R. E. DuBroff, "Near field measurements to predict the electromagnetic emission of integrated circuits," *IEEE Transactions on Electromagnetic Compatibility*, Vol. 53, No. 4, Nov. 2011.
7. Fernandez Lopez, P., A. Ramanujan, Y. Vives Gilabert, C. Arcambal, A. Louis, and B. Mazari, "A radiated emission model compatible to a commercial electromagnetic simulation tool," *20th International Zurich Symposium on Electromagnetic Compatibility*, 2009.
8. Fernández López, P., C. Arcambal, D. Baudry, S. Verdeyme, and B. Mazari, "Simple electromagnetic modeling procedure: From near-field measurements to commercial electromagnetic simulation tool," *IEEE Transactions on Instrumentation and Measurement*, Vol. 59, No. 12, Dec. 2010.
9. Huang, Q., D. Pai, K. Rao, A. Mohan, J. Vutukury, C.-M. Nieh, J. Fan, and J. Rajagopalan, "Accurate prediction and mitigation of EMI from high-speed noise sources using full wave solver," *IEEE International Symposium on Electromagnetic Compatibility, Signal & Power Integrity (EMC+SIPI)*, 22–26, Jul. 2019.
10. Liu, E.-X., W.-J. Zhao, B. Wang, S. Gao, and X.-C. Wei, "Near-field scanning and its applications," *IEEE International Symposium on Electromagnetic Compatibility & Signal/Power Integrity (EMCSI)*, 2017.
11. Alaeddin, A., M. Kadi, and H. Shall, "Modeling of the coupling phenomenon between a transmission line and a near-field excitation," *International Conference on Microelectronics (ICM)*, IEEE, 978-1-4799-3570-3, Dec. 2013.
12. Baudry, D., C. Arcambal, A. Louis, B. Mazari, and P. Eudeline, "Applications of the near-field techniques in EMC investigations," *IEEE Transactions on Electromagnetic Compatibility*, Vol. 49, No. 3, 485–493, Aug. 2007.
13. Shall, H., Z. Riah, and M. Kadi, "A 3-D near-field modeling approach for electromagnetic interference prediction," *IEEE Transactions on Electromagnetic Compatibility*, Vol. 56, No. 1, 102–112, Feb. 2014.
14. Shall, H., K. Alameh, Z. Riah, A. Alaeddine, and M. Kadi, "A tridimensional radiated emission model based on an improved near field scan technique," *First International Conference on Green Energy ICGE*, IEEE, 2014.
15. Ren, X., P. Maheshwari, Y.-J. Zhang, V. Khilkevich, J. Fan, Y. Zhou, Y. Bai, and X. Yu, "The impact of near-field scanning size on the accuracy of far-field estimation," *IEEE International Symposium on Electromagnetic Compatibility (EMC)*, 2014.
16. Zhang, L., L. Zhang, B. Wang, S. Liu, and C. Papavassiliou, "Hybrid prediction method for the electromagnetic interference characteristics of printed circuit boards based on the equivalent dipole

model and the finite-difference time-domain method," *IEEE Access (Volume: 6), Special Section On Data-Driven Monitoring, Fault Diagnosis And Control Of Cyber-Physical Systems*, 6520–6529, Dec. 13, 2017.

17. Zhang, J., K. W. Kam, J. Min, V. V. Khilkevich, D. Pommerenke, and J. Fan, "An effective method of probe calibration in phase-resolved near-field scanning for EMI application," *IEEE Transactions on Instrumentation and Measurement*, Vol. 62, No. 3, 648–658, Mar. 2013.
18. Zhao, W.-J., B.-F. Wang, E.-X. Liu, H. B. Park, H. H. Park, E. Song, and E.-P. Li, "An effective and efficient approach for radiated emission prediction based on amplitude-only near-field measurements," *IEEE Transactions on Electromagnetic Compatibility*, Vol. 54, No. 5, 1186–1189, 2012.
19. Kwak, K., J. Kim, T.-I. Bae, K. Hong, and H. Kim, "Comparison and application of two approaches extracting equivalent dipole arrays of an IC from measured near-field magnitude data," *IEEE Electrical Design of Advanced Packaging and Systems Symposium (EDAPS)*, 2018.
20. Kwak, K., J. Kim, T.-I. Bae, K. Hong, and H. Kim, "Extraction of equivalent array dipole-moments model from only magnitude data of near-field scan," *2017 Asia-Pacific International Symposium on Electromagnetic Compatibility (APEMC)*, Seoul, Korea, Jun. 20–23, 2017.
21. Shu, Y.-F., X.-C. Wei, R. Yang, and E.-X. Liu, "An iterative approach for EMI source reconstruction based on phaseless and single-plane near-field scanning," *IEEE Transactions on Electromagnetic Compatibility*, Vol. 60, No. 4, 937–944, Aug. 2018.
22. Li, L., J. Pan, C. Hwang, and J. Fan, "Radiation noise source modeling and application in near-field coupling estimation," *IEEE Transactions on Electromagnetic Compatibility*, Vol. 58, No. 4, 1314–1321, Aug. 2016.
23. Huang, Q., F. Zhang, T. Enomoto, J. Maeshima, K. Araki, and C. Hwang, "Physics based dipole moment source reconstruction for RFI on a practical cell phone," *IEEE Transactions on Electromagnetic Compatibility*, Vol. 59, No. 6, 1693–1700, 2017.
24. Vives-Gilavert, Y., C. Arcambal, A. Loius, F. Daran, P. Eudeline, and B. Mazari "Modeling magnetic radiations of electronic circuits using near-field scanning method," *IEEE Transactions on Electromagnetic Compatibility*, Vol. 49, No. 3, 391–400, Aug. 2007.
25. Leseigneur, C., P. Fernández López, C. Arcambal, D. Baudry, and A. Louis, "Near-field coupling model between electronic systems and a transmission line," *2010 IEEE International Symposium on Electromagnetic Compatibility*, Jul. 2010.
26. He, W., "Characterizing near-field circuit board radiation using crossed electric and magnetic dipole sources," M. Eng. Thesis, Missouri Univ. Sci. Technol., Rolla, MO, 2010.
27. Fernandez-Lopez, P., C. Arcambal, D. Baudry, S. Verdeyme, and B. Marzari, "Radiation modeling and electromagnetic simulation of an active circuit," *EMC Compo. 09*, 2009.
28. Shall, H., Z. Riah, and M. Kadi, "Prediction of electromagnetic interferences between components and transmission lines," *Electromagnetic Compatibility of Power Systems*, IEEE, Sep. 2012.
29. Pan, J., L. Li, X. Gao, and J. Fan, "Application of dipole-moment model in EMI estimation," *IEEE International Symposium on Electromagnetic Compatibility*, Aug. 2015.
30. Yu, Z., J. A. Mix, S. Sajuyigbe, K. P. Slattery, and J. Fan, "An improved dipole-moment model based on near-field scanning for characterizing near-field coupling and far-field radiation from an IC," *IEEE Transactions on Electromagnetic Compatibility*, Vol. 55, No. 1, 97–108, 2013.
31. Yu, Z., J. Koo, J. A. Mix, K. Slattery, and J. Fan, "Extracting physical IC models using near-field scanning," *IEEE International Symposium on Electromagnetic Compatibility*, Jul. 2010.
32. Tong, X., D. W. P. Thomas, A. Nothofer, P. Sewell, and C. Christopoulos, "Modeling electromagnetic emissions from printed circuit boards in closed environments using equivalent dipoles," *IEEE Transactions on Electromagnetic Compatibility*, Vol. 52, No. 2, 462–470, May 2010.
33. Liu, W., Z. Yan, and W. Zhao, "Extraction of equivalent dipole-moment model based on improve mapped matrix," *2016 11th International Symposium on Antennas, Propagation and EM Theory (ISAPE)*, 2016.

34. Fan, J., "Near-field scanning for EM emission characterization," *2015 IEEE Electromagnetic Compatibility Magazine*, Vol. 4, Quarter 3, 2015.
35. Tan, X., X. Li, and J. Mao, "A hybrid method for calculating dipole moment model from near-field scanning," *IEEE International Conference on Microwave and Millimeter Wave Technology (ICMMT)*, 2016.
36. Buchanan, W. J. and N. K. Gupta, "Prediction of electric fields from conductors on a PCB by 3D Finite-Difference Time-Domain (FDTD) method," *Eng. Sci. Edu. J.*, Vol. 4, No. 4, 177–182, Aug. 1995.
37. Ravelo, B. and Y. Liu, "Computation of transient near-field radiated by electronic devices from frequency data," *Fourier Transform Applications*, Ch. 1, 3–26, M. Salih, Ed., InTech, Rijeka, Croatia, Apr. 2012.
38. Jauregui, R., P. I. Riu, and F. Silva, "Transient FDTD simulation validation," *Proc. IEEE Int. Symp. Electromagn. Compact.*, Vol. 25–30, 257–262, Fort Lauderdale, FL, USA, Jul. 2010.
39. Hansen, T. B. and A. D. Yaghjian, "Planar near-field scanning in the time domain, Part 2: Sampling theorems and computation schemes," *IEEE Trans. Antennas Propag.*, Vol. 42, No. 9, 1280–1291, Sep. 1994.
40. Edwards, R. S., A. C. Marvin, and S. J. Porter, "Uncertainty analyses in the finite-difference time-domain method," *IEEE Transactions on Electromagnetic Compatibility*, Vol. 52, No. 1, 155–163, Feb. 2010.
41. Ravelo, B., Y. Liu, and A. K. Jastrzebski, "PCB near-field transient emission time-domain model," *IEEE Transactions on Electromagnetic Compatibility*, Vol. 57, No. 6, 1320–1328, Dec. 2015.
42. Liu, Y., B. Ravelo, and A. K. Jastrzebski, "Time-domain magnetic dipole model of PCB near-field emission," *IEEE Transactions on Electromagnetic Compatibility*, Vol. 58, No. 5, 1561–1569, 2016.
43. Huang, Q., Y. Liu, L. Li, Y. Wang, C. Wu, and J. Fan, "Radio frequency interference estimation using transfer function based dipole moment model," *2018 IEEE International Symposium on Electromagnetic Compatibility and 2018 IEEE Asia-Pacific Symposium on Electromagnetic Compatibility (EMC/APEMC)*, 2018.
44. Zhang, J., D. Pommerenke, and J. Fan, "Determining equivalent dipoles using a hybrid source-reconstruction method for characterizing emissions from integrated circuits," *IEEE Transactions on Electromagnetic Compatibility*, Vol. 59, No. 2, 567–575, 2017.
45. Huang, Q., Y. Chen, C. Hwang, and J. Fan, "Machine learning based source reconstruction for RF desense," *IEEE Transactions on Electromagnetic Compatibility*, Vol. 60, No. 6, 1640–1647, Dec. 2018.
46. Benyoubi, F., L. Pichon, M. Bensetti, Y. Le Bihan and M. Feliachi, "An efficient method for modeling the magnetic field emissions of power electronic equipment from magnetic near field measurements," *IEEE Transactions on Electromagnetic Compatibility*, Vol. 59, No. 2, 609–617, Apr. 2017.
47. Wu, C., Z. Sun, Q. Huang, Y. Wang, J. Fan, and J. Zhou, "A method to extract physical dipoles for radiating source characterization and near field coupling estimation," *IEEE International Symposium on Electromagnetic Compatibility, Signal & Power Integrity (EMC+SIPI)*, 2019.
48. Liu, W., Z. Yan, J. Wang, Z. Min, and Z. Ma, "An improved equivalent dipole moment source model based on regularization optimization method for near field-far field conversion," *IEEE Access*, Vol. 8, 42504–42518, Mar. 2020.
49. Tong, X., D. W. P. Thomas, A. Nothofer, P. Sewell, and C. Christopoulos, "Modeling electromagnetic emissions from printed circuit boards in closed environments using equivalent dipoles," *IEEE Transactions on Electromagnetic Compatibility*, Vol. 52, No. 2, 462–470, May 2010.
50. Pan, J., G. Li, Y. Zhou, Y. Bai, X. Yu, Y. Zhang, and J. Fan, "Measurement validation of the dipole-moment model for IC radiated emission," *IEEE International Symposium on Electromagnetic Compatibility*, Aug. 5–9, 2013.
51. Pan, J., H. Wang, X. Gao, C. Hwang, E. Song, H.-B. Park, and J. Fan, "Radio-frequency interference estimation using equivalent dipole-moment models and decomposition method based on reciprocity," *IEEE Transactions on Electromagnetic Compatibility*, Vol. 58, No. 1, 75–84, Feb. 2016.

52. Kwak, K., J. Kim, T.-I. Bae, K. Hong, and H. Kim, "Extraction of equivalent array dipole-moments model from only magnitude data of near-field scan," *2017 Asia-Pacific International Symposium on Electromagnetic Compatibility (APEMC)*, Seoul, Korea, Jun. 20–23, 2017.
53. Wang, H., V. Khilkevich, Y.-J. Zhang, and J. Fan, "Estimating radiofrequency interference to an antenna due to near-field coupling using decomposition method based on reciprocity," *IEEE Transactions on Electromagnetic Compatibility*, Vol. 55, No. 6, 1125–1131, Dec. 2013.
54. Li, L., J. Pan, C. Hwang, G. Cho, H. Park, Y. Zhang, and J. Fun, "Near-field coupling estimation by source reconstruction and Huygens's equivalence principle," *Proc. IEEE Int. Symp. Electomagn. Compat.*, 324–329, Santa Clara, USA, Mar. 2015.
55. Li, L., J. Pan, C. Hwang, G. Cho, H. Park, Y. Zhang, and J. Fan, "Measurement validation for radio-frequency interference estimation by reciprocity theorem," *IEEE International Symposium on Electromagnetic Compatibility*, 2015.